ITECKNE

Exoskeleton for ankle joint flexion/ extension rehabilitation

Exoesqueleto para rehabilitación de la flexión/extensión de la articulación del tobillo

José Luis Sarmiento-Ramos[1]   ; Juan Camilo Suárez-Galvis[1]; Valentina Grisales-Muñoz[1]

[1]Universidad Manuela Beltrán, Bucaramanga, Colombia. jose.sarmiento@docentes.umb.edu.co; juan.cuarez@academia.umb.edu.co; valentina.grisales@academia.umb.edu.co

Abstract: This work presents the modelling, design, construction, and control of an exoskeleton for ankle joint flexion/extension rehabilitation. The dynamic model of the ankle flexion/extension is obtained through Euler-Lagrange formulation and is built in Simulink of MATLAB using the non-linear differential equation derived from the dynamic analysis. An angular displacement feedback PID controller, representing the human neuromusculoskeletal control, is implemented in the dynamic model to estimate the joint torque required during ankle movements. Simulations are carried out in the model for the ankle flexion/extension range of motion (ROM), and the results are used to select the most suitable actuators for the exoskeleton. The ankle rehabilitation exoskeleton is designed in SolidWorks CAD software, built through 3D printing in polylactic acid (PLA), powered by two on-board servomotors that deliver together a maximum continuous torque of 22 [kg·cm], and controlled by an Arduino board that establishes Bluetooth communication with a mobile app developed in MIT App Inventor for programming the parameters of the rehabilitation therapies. The result of this work is a lightweight ankle exoskeleton, with a total mass of 0.85 [kg] including actuators (servomotors) and electronics (microcontroller and batteries), which can be used in telerehabilitation practices guaranteeing angular displacement tracking errors under 10%.

Keywords: rehabilitation robotics; wearable robotics; plantarflexion; dorsiflexion; model; Euler-Lagrange; control; Arduino.

Resumen: Este trabajo presenta el modelado, diseño, construcción y control de un exoesqueleto para rehabilitación de la flexión/extensión de la articulación del tobillo. El modelo dinámico de la flexión/extensión del tobillo es obtenido por medio de la formulación de Euler-Lagrange y es construido en Simulink de MATLAB usando la ecuación diferencial no-lineal derivada del análisis dinámico. Un controlador PID de realimentación del desplazamiento angular, representando el control neuromusculoesquelético humano, es implementado en el modelo dinámico para estimar el torque articular requerido durante los movimientos del tobillo. Se hacen simulaciones en el modelo para el rango de movimiento (ROM) de la flexión/extensión del tobillo, y los resultados son usados para seleccionar el actuador más adecuado para el exoesqueleto. El exoesqueleto para rehabilitación del tobillo es diseñado en el *software* CAD SolidWorks, construido por impresión 3D en ácido poliláctico (PLA), accionado por dos servomotores que entregan juntos un torque continuo máximo de 22 [kg·cm], y controlado por una placa Arduino que establece comunicación Bluetooth con un aplicativo móvil desarrollado en MIT App Inventor para la programación de los parámetros de las terapias de rehabilitación. El resultado de este trabajo es un exoesqueleto liviano de tobillo, con una masa total de 0.85[kg] incluyendo actuadores (servomotores) y electrónica (microcontrolador y baterías), el cual puede ser usado en prácticas de telerehabilitación, garantizando errores de seguimiento del desplazamiento angular por debajo del 10%.

Palabras clave: robótica de rehabilitación; robótica vestible; plantiflexión; dorsiflexión; modelo; Euler-Lagrange; control; Arduino.

Exoskeleton for ankle joint flexion/extension rehabilitation - J. Sarmiento Ramos, J. Suárez Galvis, and V. Grisales Muñoz

105

1. INTRODUCTION

Most rehabilitation therapies require accompaniment of physiotherapists or physiologists to perform repetitive movements and exercises in the affected joint. The application of wearable robotics to the medical field, particularly of rehabilitation exoskeletons, constitutes as a good cost-benefit solution to support conventional rehabilitation services [1]; especially given the current worldwide situation due to COVID-19, where physical contact should be avoided, and where telemedicine-based techniques are booming.

The ankle joint is the final component of the lower body and works in conjunction with the foot in daily activities such as bipedal stance and locomotion [2]. The functions of the ankle are providing stability to bear body weight during stance and participate in the advance of the body over the fixed foot during locomotion. Due to the high loads the ankle must withstand and its supporting structures, it is considered the lower body joint where most injuries take place. Ankle sprain is one of the most frequent musculoskeletal injuries in general population and athletes, being up to 30% of sports injuries [3]. Epidemiological incidence data indicates that one ankle sprain occurs daily for every then thousand people, causing considerable loss of time due to disability, and a high cost in medical care [4].

Ankle and lower-limb exoskeletons developed in previous works have focused mainly on gait rehabilitation, walking assistance for disabled people, human gait augmentation, and reduction of the metabolic cost of walking. However, exoskeletons dedicated exclusively to ankle joint range of motion (ROM) recovery and rehabilitation in neuromuscular injuries have not been widely explored.

Gait rehabilitation and assistance exoskeletons are active structures powered by electro-mechanical devices such as DC motors, series-elastic actuators (SEA), and pneumatic actuators, to provide the required torque or force to move the foot according to the gait cycle. Ferris *et al.* [5] developed an ankle-foot orthosis for walking assistance of paraplegics powered by two pneumatic artificial muscles, one located at the back of the lower leg aligned with the Achilles tendon and the other one at the front aligned with the Tibialis Anterior. Witte *et al.* [6] designed and built two lightweight gait assisting exoskeletons powered by Bowden cables coupled to an off-board DC motor, whose torque was controlled using a combination of proportional feedback and damping injection with iterative learning during walking tests. Yu *et al.* [7] developed a modular knee-ankle wearable robot for gait impairments assistance, powered by a novel actuator composed of a DC motor driving a ball screw through a torsional spring assembly and a pair of spur gear, controlled by a high-fidelity force PD controller. Shorter *et al.* [8] designed a portable pneumatically powered ankle-foot orthosis for enhancing walking function, gait training in physical therapies, and providing external power-assisted therapy modalities for improving strength and ROM.

Exoskeletons for human gait augmentation and reduction of the metabolic cost of walking consists of passive and active alternatives. Passive exoskeletons do not require and external power supply, since they use passive elements, such as springs and clutches, to store energy and deliver it at a given time. Active exoskeletons use the same electro-mechanical devices as gait rehabilitation and assistance exoskeletons, and thus require a power supply to drive those actuators. Bougrinat *et al.* [9] developed a lightweight ankle exoskeleton for human walking augmentation using a DC motor, a gearbox and Bowden cables to transmit the mechanical force from the actuation unit attached to the waist to the carbon fiber struts fixed on the foot, to create an assistive ankle plantarflexion torque. Wang *et al.* [10] built a passive spring-actuated ankle-foot exoskeleton to assist human gait and lengthen its duration by mechanically enhancing walking efficiency. The exoskeleton was equipped with a smart clutch to identify gait stages and be able to deliver the energy stored in a suspended spring behind the human calf muscles, to provide toe-off energy for the swing phase. Leclair *et al.* [11] developed a passive ankle exoskeleton for walking assistance using a flexible air-spring to harness gait energy and compliment the human ankle torque at push-off. Liu *et al.* [12] built an active ankle exoskeleton to create high power assistance for push-off during gait cycle. The exoskeleton was powered by a lightweight DC motor and designed to provide a high peak power assistance with a low peak power motor. This was done by injecting energy of the actuator during relatively long time in stance phase and releasing it during relatively short time in swing phase.

This work presents the modelling, design, construction, and control of a rehabilitation exoskeleton for the ankle joint flexion/extension. The dynamic model developed herein constitutes as a powerful tool to estimate joint torques in the ankle for any ROM, velocity, reference trajectory and anthropometric configuration of the patient (body mass and height), and therefore becomes a great assistance to select the most suitable actuators for the exoskeleton. The dynamic modeling presented herein is of great importance since it can be extrapolated to the analysis of the fundamental movements of any joint of the human body. The ankle rehabilitation exoskeleton developed in this work is built through 3D printing in polylactic acid (PLA) for light weight and is powered by two on-board servomotors that are controlled by an Arduino board which is commanded by a mobile app where the patient or physiotherapist can introduce the parameters of the rehabilitation therapy such as ROM, repetitions, and velocity.

This paper is organized as follows: section 2 describes the dynamic modeling of the ankle flexion/extension through Euler-Lagrange formulation and the implementation of the dynamic model in Simulink of MATLAB in conjunction with a PID feedback controller representing the human neuromusculoskeletal control. Section 3 shows the design of the exoskeleton in SolidWorks 3D CAD software and its constructions through 3D printing. The electronic circuit, control system and mobile app of the exoskeleton are exposed in section

4. Finally, section 5 presents tracking performance tests of the exoskeleton for load torque situations, ROMs and velocities, and the results are evaluated in terms of the relative maximum error, to present the final conclusions of the work in section 6.

2. DYNAMIC MODELING

The dynamic model of the ankle flexion/extension is obtained through Euler-Lagrange formulation considering the system represented in Fig. 1, where the foot is modeled as a rigid bar of length L, mass m, and proximal gravity center l. The origin of the coordinate system is fixed at the ankle joint, and the foot is flexed at an angle θ.

Fig.1. REPRESENTATION OF THE FOOT FOR DYNAMIC MODELING
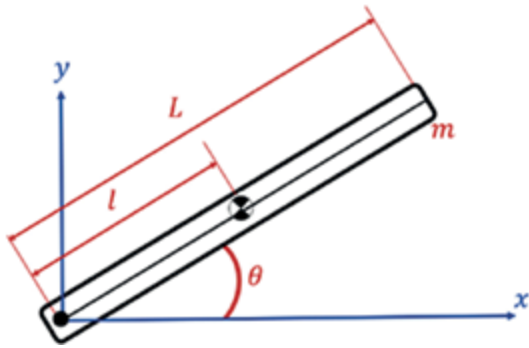
Source: The authors.

The Lagrangian L is defined as the difference between the system's kinetic energy T and potential energy V (1)

$$L = T - V \quad (1)$$

The system's kinetic energy is established in (2), where J is the moment of inertia, and $\dot{\theta}$ the angular velocity of the foot. The system's potential energy is shown in (3).

$$T = \frac{1}{2} ml^2 \dot{\theta}^2 + \frac{1}{2} J \dot{\theta} \quad (2)$$

$$V = mgl sin\theta \quad (3)$$

Substituting (2) and (3) into (1) results in the system's Lagrangian:

$$L = \frac{1}{2} ml^2 \dot{\theta}^2 + \frac{1}{2} J \dot{\theta} - mgl sin\theta \quad (4)$$

Euler-Lagrange formulation is established as shown in (5), where k are the system's degrees of freedom (DOF), q_k the set of generalized coordinates, and Q_k the set of external forces (non-conservative). In the model there is only one DOF related to the ankle flexion/extension. The external forces consist of the joint torque T and the viscous damping. Considering this,

the Euler-Lagrange formulation for the system turns into (6), where b is the ankle viscous damping coefficient.

$$\frac{d}{dt}\left(\frac{\partial L}{\partial \dot{q}_k}\right) - \frac{\partial L}{\partial q_k} = Q_k \quad (5)$$

$$\frac{d}{dt}\left(\frac{\partial L}{\partial \dot{\theta}}\right) - \frac{\partial L}{\partial \theta} = T - b\dot{\theta} \quad (6)$$

Euler-Lagrange formulation (6) is solved for the Lagrangian derivates resulting in the non-linear second-order differential equation (7) that describes the dynamics of the ankle flexion/extension.

$$ml^2 \ddot{\theta} + J\ddot{\theta} + mgl cos\theta = T - b\dot{\theta} \quad (7)$$

To build the dynamic model, (7) is solved for the highest order derivative $\ddot{\theta}$ resulting in (8).

$$\ddot{\theta} = \frac{1}{ml^2 + J}\left[T - b\dot{\theta} - mgl cos\theta\right] \quad (8)$$

The ankle flexion/extension model is built in Simulink of MATLAB using the non-linear second-order differential equation (8) as shown in Fig. 2. The input to the model is the joint torque, and the outputs are the foot's angular displacement, velocity, and acceleration in [rad], [rad/s] and [rad/s^2] respectively. Signal saturators are installed to restrict the ankle flexion/extension ROM according to the values reported in literature [2] (Table I). These saturators are applied to the ankle's angular displacement through a SPDT (single pole, double throw) switch that is automatically commutated by a sign function block depending on the performed movement of the foot.

Fig.2. DYNAMIC MODEL OF THE ANKLE FLEXION/EXTENSION BUILT IN SIMULINK
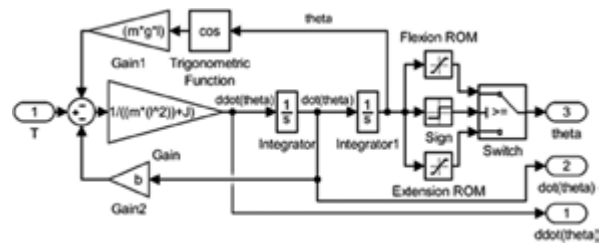
Source: The authors.

Table I.
ANKLE JOINT ROMs

Movement	ROM [°]
Flexion (plantarflexion)	50
Extension (dorsiflexion)	30

Source: The authors.

The parameters of the ankle flexion/extension dynamic model are obtained from anthropometric studies [13][14] and are listed in Table II. The mass of the foot is function of the patient's body mass M in [kg], the length of the foot is function of the patient's height H in [m], and the proximal gravity center and radius of gyration are function of the length of the foot.

Table II.
PARAMETERS OF THE DYNAMIC MODEL OF THE ANKLE FLEXION/
EXTENSION

Parameter	Symbol	Value	Units
Mass of the foot	m	0.0145·M	[kg]
Length of the foot	L	0.152·H	[m]
Proximal gravity center	l	0.5·L	[m]
Radius of gyration of the foot	K	0.690·L	[m]
Moment of inertia of the foot	J	m·k²	[Kg·m²]
Viscous damping coefficient	b	0.1	[N·m·s]
Gravity	g	9.81	[m/s²]

Source: The authors.

To perform simulations in the ankle flexion/extension dynamic model for a given reference trajectory, an angular displacement feedback PID controller is implemented in Simulink as shown in Fig. 3. This feedback controller represents the human natural neuromusculoskeletal control [1], where the input signal is the tracking error, defined as the difference between the reference trajectory and the real displacement of the limb, and the output signal is the human joint torque required to produce the desired movement. The output of the PID controller is fed into the ankle flexion/extension dynamic model of Fig. 2, which is packed in a Simulink subsystem block as depicted in Fig. 3. Since the dynamic model works with angular position, velocity, and acceleration in [rad], [rad/s] and [rad/s²] respectively, gain blocks are installed to perform unit conversion. The reference trajectory is converted from [°] to [rad] before the calculation of the tracking error is done, and the outputs of the model are converted to [°], [°/s] and [°/s²] for plotting purposes.

Fig. 3. PID CONTROLLER IMPLEMENTED IN THE ANKLE FLEXION/EXTENSION DYNAMIC MODEL IN SIMULINK
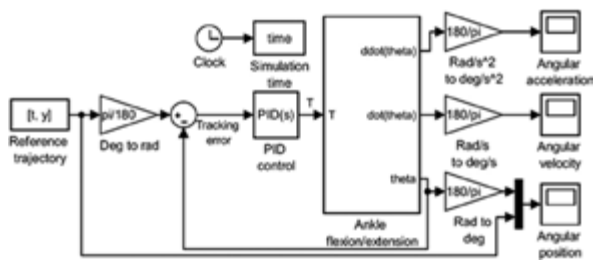
Source: The authors.

PID control is a classic strategy based on three gains: proportional, integral, and derivative. The proportional gain increases system's response, the integral gain reduces steady-state error, and the derivate gain reduces the tracking

error by responding to its evolution over time [15]. The transfer function of the PID controller is shown in (9), where K_p, K_i and K_d are the proportional, integral, and derivate gains, respectively. The PID controller was experimentally tuned in the ankle flexion/extension dynamic model until achieving the best tracking performance, obtained with a PD controller where $K_p = 100$ and $K_d = 10$.

$$PID(s) = K_P + \frac{K_i}{s} + K_d s \quad (9)$$

The dynamic model is simulated considering the average Colombian adult anthropometric data (body mass and height) [16] and using sinusoidal waves as reference trajectories [17] with the maximum ankle ROMs specified in Table I. Graphical simulation results are shown in Fig. 4 and 5 for a 50° flexion and 30° extension, respectively. Each figure consists of two plots related as follows: (a) angular displacement, where the dotted line indicates the reference trajectory and the solid line the displacement of the foot, and (b) the required torque for the execution of the desired movement. From the angular displacement plots can be seen that the dynamic model achieves precise tracking of the reference trajectories. From the joint torque plots can be observed that the maximum torque takes an approximate value of 13 [kg·cm] and is obtained in the position where $\theta = 0$ [°] relative to the horizontal axis (x axis of Fig. 1, fully horizontal foot), and as the foot flexes or extends the torque decreases. This is due to a reduction of the perpendicular distance between the weight vector of the foot, located at its center of gravity, and the ankle joint.

The dynamic model constitutes as a powerful to estimate ankle joint torques for any ROM, velocity, reference trajectory and anthropometric configuration of the patient (body mass and height), and thus, becomes a great assistance to select the most suitable actuators for the exoskeleton. The dynamic modeling presented herein through Euler-Lagrange formulation can be extrapolated to the analysis of the fundamental movements of any joint of the human body [18][19].

Fig.4. ANKLE 50[°] FLEXION: (a) ANGULAR DISPLACEMENT AND (b) TORQUE
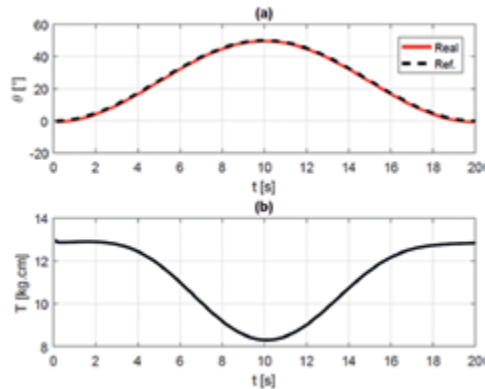
Source: The authors.

Fig. 5. ANKLE 30[°] EXTENSION: (a) ANGULAR DISPLACEMENT AND (b) TORQUE
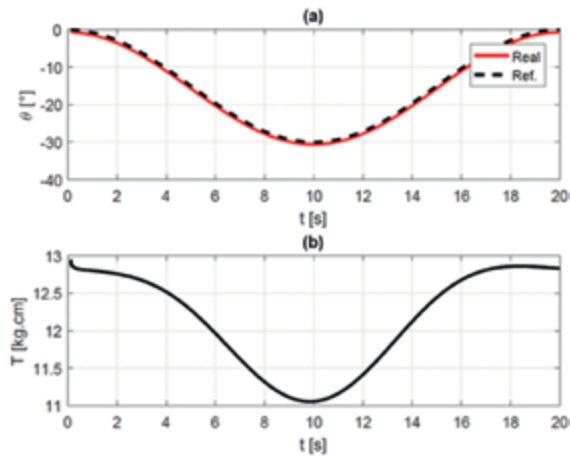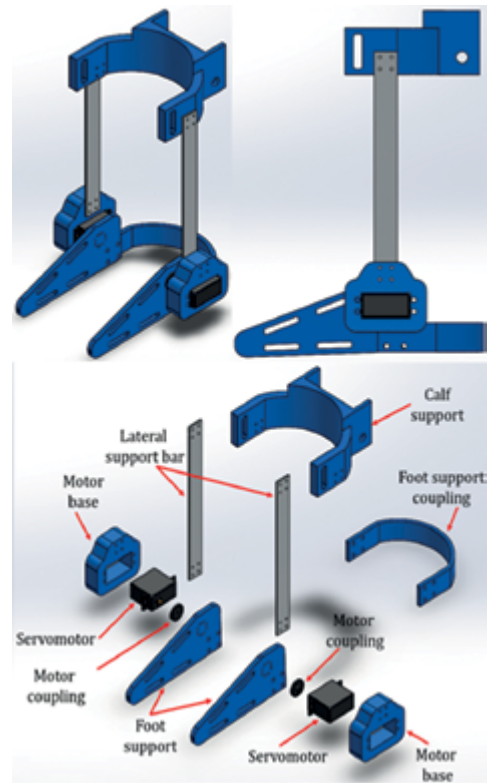

Source: The authors.

3. EXOSKELETON DESIGN AND CONSTRUCTION

The ankle exoskeleton considered in this work has only one degree of freedom (DOF) related to the flexion/extension. To execute these movements the exoskeleton actuators must satisfy two requirements: (1) supply the ankle flexion/extension ROMs (Table I), and (2) supply the required joint torque. The maximum joint torque, as obtained from the simulation results of the previous section, is of approximately 13 [kg·cm] considering the average Colombian adult anthropometric data. The maximum torque is multiplied by a safety factor of 1.5 considering that its estimation was done with average anthropometric data and with the intention that the exoskeleton can be used in people with greater body mass and/or height than the average, resulting in a maximum torque of 19.5 [kg·cm].

To satisfy the ROM and torque requirements, two MG996r servomotors are selected as the exoskeleton actuators. Each motor delivers a maximum torque of 11 [kg·cm], resulting in a maximum continuous torque of 22 [kg·cm] when they are placed together in the ankle joint.

The exoskeleton is designed in SolidWorks CAD software as shown in Fig. 6, considering the anthropometric data of Colombian adults [16]. As seen in the exploded view, the exoskeleton consists of seven elements: (1) calf support, to contain the electronics and serve as a fixing element to the patient's leg; (2) lateral bar, fixed to the calf support to support the motor base; (3) motor base, fixed to the lateral bar to support the servomotors; (4) servomotor MG996r; (5) motor coupling, to connect the motor shaft with the foot support; (6) foot support, to hold the foot through adjustable straps and guarantee the execution of the flexion/extension; and (7) foot support coupling, to connect the two foot support elements for a synchronized motion.

Fig.6. ISOMETRIC, SIDE, AND EXPLODED VIEWS OF THE ANKLE REHABILITATION EXOSKELETON IN SOLIDWORKS

Source: The authors.

To guarantee rigid support and lightweight, most parts of the exoskeleton (calf support, motor base, foot support and foot support coupling) are built through 3D printing in PLA, and the lateral support bars are made of aluminum. The manufacturing and assembly of the different elements results in the ankle exoskeleton shown in Fig.7, whose total mass is 0.85 [kg] including servomotors, electronics, and batteries. The ankle exoskeleton is located on the patient's lower leg and fixed to the calf and foot through adjustable straps to execute the rehabilitation therapies.

Fig.7. ANKLE FLEXION/EXTENSION REHABILITATION EXOSKELETON

Source: The authors.

Exoskeleton for ankle joint flexion/extension rehabilitation - J. Sarmiento Ramos, J. Suárez Galvis, and V. Grisales Muñoz

109

## 4. EXOSKELETON CIRCUIT AND CONTROL

The exoskeleton electronic circuit is shown in Fig. 8 and is composed of: Arduino UNO microcontroller, MG996r servomotors, HC05 Bluetooth module, MT3608 voltage booster module, battery holder for two Li-ion 18650 batteries, battery holder for four rechargeable batteries, pushbutton, LED, and 1k resistor. Additionally, there is a charging circuit for the Li-ion 18650 batteries that consists of a TP4065 charging module and a battery holder.

The Arduino UNO microcontroller is powered by four rechargeable batteries and is used to control the servomotors according to the rehabilitation therapy parameters introduced in the mobile app. The communication between the cellphone (mobile app) and the Arduino is done through Bluetooth connection supplied by the HC05 module, which is connected to the TX and RX Arduino terminals. The pushbutton gives the command to the Arduino board to start or stop the rehabilitation therapy and its status is visualized in the LED. The MG996r servomotors are powered by two Li-ion 18650 batteries (of 4.2 [V] DC and 6800 [mAh]) through the MT3068 voltage booster module, which raises the voltage to 6 [V] to guarantee the motor torque requirements. Separate power supplies are considered for the control stage and power stage of the exoskeleton (Arduino board and servomotors, respectively), to not compromise the current supply to the motors and guarantee their output torque.

The exoskeleton control system is programmed in Arduino as seen in the flowchart of Fig. 9. The code begins with the confirmation of Bluetooth connection between the mobile device and the HC05 module. Once the connection is guaranteed, the Arduino reads three therapy parameters entered by the patient or therapist in the mobile app: (1) flexion/extension ROM, (2) number of repetitions of the movement, and (3) velocity of the rehabilitation therapy. When these parameters are entered, the exoskeleton waits for the command of the pushbutton to start the therapy. If the pushbutton is off, the exoskeleton remains in the 0[°] position (fully horizontal foot). Once the button is pressed, the internal loops of the control algorithm generate the movement of the servomotors, using Arduino's <Servo.h> library, according to the parameters introduced in the mobile app. When the therapy is finished, the exoskeleton stops in the fully horizontal position of the foot. The pushbutton works as a physical start/stop button since it enables or disables the movement of the motors in the control algorithm as seen in the flowchart of Fig. 9. In that respect, the pushbutton is considered a safety feature of the exoskeleton, acting as a physical emergency button for the patient whenever he feels pain or discomfort. The controller, from the perspective of movement, is considered open-loop since no feedback is generated from the actual position of the foot. However, the positioning of the servomotors is carried out taking advantage of their internal closed-loop control and its programming through <Servo.h> library.

For entering the rehabilitation therapy parameters, an Android mobile app is developed using MIT App Inventor. The app, as shown in Fig. 10, consists of two buttons to connect or disconnect the Bluetooth communication with the HC05 module, six buttons for selecting the ankle flexion/extension ROM from 5 to 30[°], nine buttons for selecting the numbers of repetitions between one to nine, and three buttons for selecting the speed of the therapy. Within the mobile app there is an additional safety feature for the patient, since if the button to disconnect the Bluetooth communication is pressed, then the control algorithm will stop the movement of the motors.
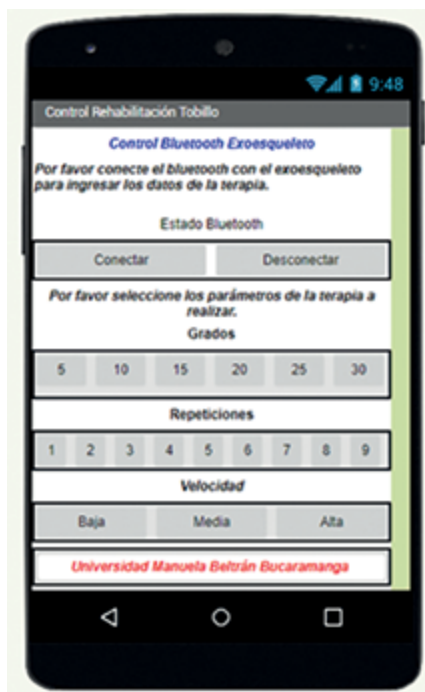
Fig. 8. EXOSKELETON ELECTRONIC CIRCUIT
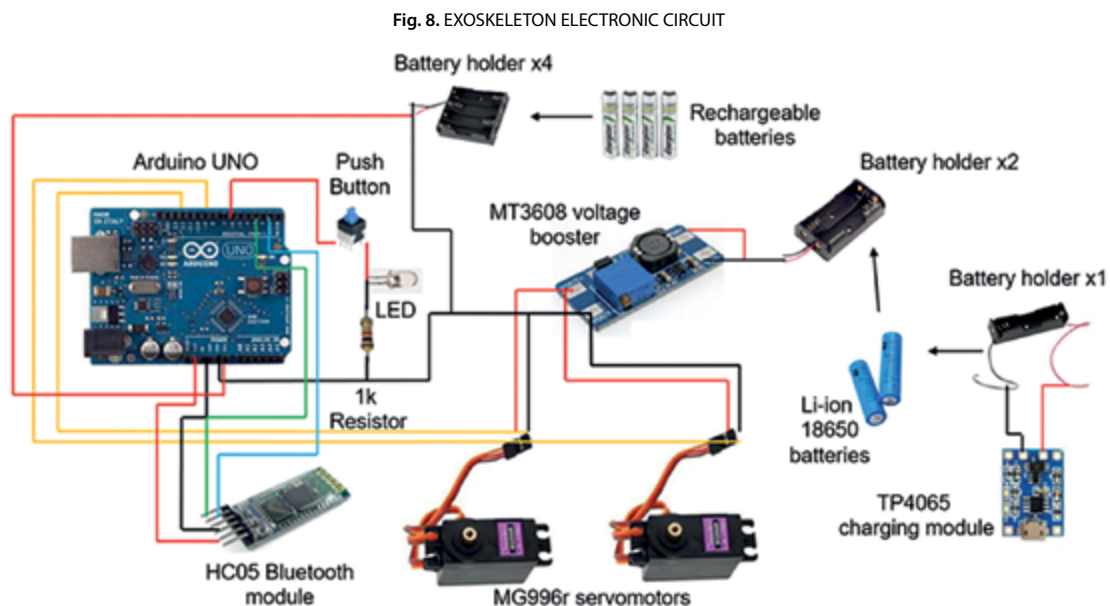
Source: The authors.

Fig. 9. FLOWCHART OF THE CONTROL ALGORITHM IN ARDUINO
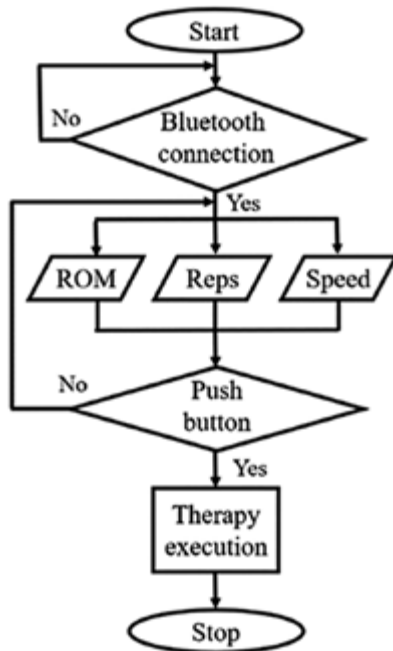
Source: The authors.

Fig.10. MOBILE APP DEVELOPED IN MIT APP INVENTOR

Source: The authors.

5. EXOSKELETON FUNCTIONAL TESTS

Functional tests of the ankle flexion/extension rehabilitation exoskeleton were performed to verify its angular displacement tracking performance under different load torque situations. The results were quantitatively evaluated considering the relative maximum error (RME) calculated using (10), where θ_d is the reference angular displacement and θ_m the measured angular position of the foot [20].

$$\%RME = \frac{\max\left|\theta_d - \theta_m\right|}{\max\left|\theta_d\right|} \quad (10)$$

Four different load torque situations were considered: the first one without load (no patient), and the other three with patients of different body masses and heights, resulting in different torque requirements according to the mass of the foot and its gravity center. The angular displacement tracking was evaluated for ankle ROMs of 5, 10, 15, 20, 25 and 30 [°], and for the three velocities configured in the mobile app. The results are summarized in Table 3, where it is observed that the largest tracking errors are obtained for the following situations: (1) for the patient with the greatest body mass and height, (2) for smaller ROMs, and (3) when the velocity is set at its slowest value. For the different situations (patients, ROMs, and velocities) the tracking errors remain under 10%.

6. CONCLUSIONS

This work presented the modelling, design, construction, and control of an ankle flexion/extension rehabilitation exoskeleton. The dynamic model of the ankle flexion/extension was obtained through Euler-Lagrange formulation and was built in Simulink of MATLAB using the non-linear differential equation obtained from the dynamic analysis, where a PID feedback control was implemented to recreate the human natural neuromusculoskeletal control. This dynamic model constitutes as a powerful tool to estimate joint torques in the ankle for any ROM, velocity, reference trajectory and anthropometric configuration of the patient (body mass and height), and therefore becomes a great assistance to select the most suitable actuators for the exoskeleton. Simulations were performed for the average Colombian adult anthropometric data and for the maximum ankle flexion/extension ROM, obtaining a maximum torque of approximately 13 [kg·cm] in the fully horizontal position of the foot.

The exoskeleton was designed in SolidWorks CAD software, and is composed of seven elements: calf support, foot supports, foot support coupling, lateral bars, motor bases, motor coupling, and two servomotors MG996r, selected considering the simulation results of the dynamic model, capable of delivering a maximum continuous torque of 22 [kg·cm]. Most elements of the exoskeleton were built trough 3D printing in PLA, while the lateral bars were manufactured in aluminum, resulting in a total mass of the exoskeleton of 0.85 [kg] including servomotors, electronics, and batteries. The exoskeleton control system was programmed in an Arduino UNO board using the <Servo.h> library to run the servomotors taking advantage of its internal closed-loop control. The Arduino establishes Bluetooth communication

through a HC05 module with a mobile app developed in MIT App Inventor, for introducing three rehabilitation therapy parameters: flexion/extension ROM, number of repetitions, and therapy speed. The conjunction of the control system and the mobile app gives the exoskeleton the potential to be used for telemedicine rehabilitation practices.

Performance tests of the exoskeleton angular displacement tracking were performed for different load torque situations (no load and patients with different body masses and heights) considering different flexion/extension ROMs and velocities, and the results were quantitatively evaluated using the relative maximum error (RME). The exoskeleton showed angular displacement tracking with RMEs under 10%. In future works it is intended to develop closed-loop control strategies to minimize the tracking error and guarantee precisely tracking of the reference rehabilitation trajectories.

Table III.
FUNCTIONAL TESTS RESULTS

Load situation	Slow velocity			Medium velocity			Fast velocity		
	θ_d [°]	θ_m [°]	% RME	θ_d [°]	θ_m [°]	% RME	θ_d [°]	θ_m [°]	% RME
No load (no patient)	5	5.5	10	5	5.5	10	5	5	0
	10	10	0	10	10	0	10	10	0
	15	15.5	3.333	15	15.5	0	15	15	0
	20	20	0	20	20	0	20	20	0
	25	25	0	25	25	0	25	25.5	2
	30	30	0	30	30	0	30	30	0
Patient 1 Body mass = 58 [kg] Height = 1.58 [m]	5	5.5	10	5	5	0	5	5.5	10
	10	11	10	10	11	10	10	10	0
	15	15.5	3.333	15	15	0	15	15	0
	20	20	0	20	21	5	20	21	5
	25	25	0	25	26	4	25	25	0
	30	31	3.333	30	29	3.333	30	31	3.333
Patient 2 Body mass = 62 [kg] Height = 1.62 [m]	5	5.5	10	5	5.5	10	5	5.5	10
	10	11	10	10	10	0	10	9.5	5
	15	16	6.667	15	16	6.667	15	16	6.667
	20	21	5	20	20	0	20	21	5
	25	26.5	6	25	26.5	6	25	26	4
	30	29	1.333	30	27	10	30	30	0
Patient 3 Body mass = 69 [kg] Height = 1.78 [m]	5	5.5	10	5	5.5	10	5	5.5	10
	10	9	10	10	9	10	10	9.5	5
	15	16.5	10	15	14	6.667	15	16	6.667
	20	21	5	20	19	5	20	21	5
	25	27	8	25	26	4	25	26	4
	30	32	6.667	30	29	1.333	30	29	1.333

Source: The authors.

7. REFERENCES

[1] M. Oluwatsin, Modelling and control of actuated lower limb exoskeletons: a mathematical application using central pattern generators and nonlinear feedback control techniques, PhD dissertation, Tshwane University of Technology, 2016.

[2] C. A. Oatis, *Kinesiology: the mechanics and pathomechanics of human movement*, 2nd Ed, USA, Lippincott Williams & Wilkin, 2009.

[3] D. F. Rincón-Cardozo, J. A. Camacho Casas, P. A. Rincón-Cardozo, and N. Sauza-Rodríguez, Approach of ankle sprain for the general physician, *Revista de la Universidad Industrial de Santander,* 47 (1), pp. 85-92, 2015. https://revistas.uis.edu.co/index.php/revistasaluduis/article/view/4684

[4] K. Moore, A. Dalley, and A. Agur, *Anatomía con orientación clínica*, 5th Ed, México, Wolters Kluwer, 2007.

[5] D. P. Ferris, J. M. Czerniecki, and B. Hannaford, An ankle-foot orthosis powered by artificial pneumatic muscles, *Journal of Applied Biomechanics*, 21 (2), pp. 189-197, 2006. DOI: https://doi.org/10.1123/jab.21.2.189

[6] K. A. Witte, J. Zhang, R. W. Jackson, and S. H. Collins, Design of two lightweight, high-bandwidth torque-controlled ankle exoskeletons, in *2015 IEEE International Conference on Robotics and Automation (ICRA)*, 2015. pp. 1123-1128. DOI: https://doi.org/10.1109/ICRA.2015.7139347

[7] H. Yu, M. Cruz, G. Chen, S. Huang, C. Zhu, E. Chew, Y. S. Ng, and N. V. Thakor, Mechanical design of a portable knee-ankle for robot, in *2013 IEEE International Conference on Robotics and Automation (ICRA)*, pp. 2183-2188, 2013. DOI: https://doi.org/10.1109/ICRA.2013.6630870

[8] K. A. Shorter, G. F. Kogler, E. Loth, W. K. Durfee, and E. T. Hsiao-Wecksler, A portable powered ankle-foot orthosis for rehabilitation, *Journal of Rehabilitation Research & Development*, 48 (4), pp. 459-472, 2011. DOI: https://doi.org/10.1682/jrrd.2010.04.0054

[9] Y. Bougrinat, S. Achiche, and M. Raison, Design and development of a lightweight ankle exoskeleton for human walking augmentation, *Mechatronics*, 64, 2019. DOI: https://doi.org/10.1016/j.mechatronics.2019.102297

[10] X. Wang, S. Guo, B. Qu, M. Song, and H. Qu, Design of a passive gait-based ankle-foot exoskeleton with self-adaptive capability, *Chinese Journal of Mechanical Engineering*, 33 (49), 2020. DOI: https://doi.org/10.1186/s10033-020-00465-z

[11] J. Leclair, S. Pardoel, A. Helal, and M. Doumit, Development of an unpowered ankle exoskeleton for walking assist, *Disability and Rehabilitation: Assistive Technology*, 2018. DOI: https://doi.org/10.1080/17483107.2018.1494218

[12] J. Liu, C. Xiong, and C. Fu, "An ankle exoskeleton using lightweight motor to create high power assistance for push-off," *Journal of Mechanisms and Robotics*, 2019. DOI: https://doi.org/10.1115/1.4043456

[13] D. A. Winter, *Biomechanics and motor control of human movement,* 4th Ed, New Jersey, John Wiley & Sons, Inc., 2009.

[14] Y. Li, C. Xu, and X. Guan, "Modeling and simulation study of electromechanically system of the human extremity exoskeleton," *Journal of Vibroengineering*, 18 (1), pp. 551-661, 2020.

[15] C. Borrás, J. L. Sarmiento, and J. F. Ortiz, "Dynamic model and control design for a nonlinear hydraulic actuator," in *ASME 2018 International Mechanical Engineering Congress and Exposition*, 2018. DOI: https://doi.org/10.1115/IMECE2018-88320

[16] R. A. Chaurand, L. R. Prado, and E. L. González, *Dimensiones antropométricas de la población latinoamericana*, México, Universidad de Guadalajara, 2007.

[17] Z. Taha, A. Abdul, M. Y. Wong, M. A. Hashem, I. M. Khairuddin, and M. A. Mohd, "Modelling and control of an upper extremity exoskeleton for rehabilitation," *IOP Conf. Series: Materials, Science and Engineering*, 114, 2016. DOI: https://doi.org/10.1088/1757-899X/114/1/012134

[18] J. L. Sarmiento-Ramos, A. P. Rojas-Ariza, and Y. Z. Rueda-Parra, "Dynamic model of flexion/extension and abduction/adduction of the shoulder joint complex," in *2021 IEEE 2nd International Congress of Biomedical Engineering and Bioengineering (CI-IB&BI)*, 2021, pp.1-4. DOI: https://doi.org/10.1109/CI-IBBI54220.2021.9626105

[19] R. A. Díaz-Suárez, L. T. Moreno-Moreno, M. A. Sanjuan-Vargas, C. A. Prada-García, and L. D. Torres, "Development of an exoskeleton for the rehabilitation of the flexo-extensor movement of the elbow", *ITECKNE*, 18 (1), pp. 46-51, 2021. DOI: https://doi.org/10.15332/iteckne.v18i1.2539

[20] C. Borrás, J. L. Sarmiento, and R. D. Guiza, "Modelling, system identification and position control based on LQR formulation for an electro-hydraulic servo system," in *ASME 2019 International Mechanical Engineering Congress and Exposition*, 2019. DOI: https://doi.org/10.1115/IMECE2019-11505